

1
2
3
4 **Influence of fine sediment on the fluidity of debris flows**

5
6 **Norifumi HOTTA^{1*}, Takahiro KANEKO², Tomoyuki IWATA³, Haruo NISHIMOTO¹**

7
8 1 Faculty of Life and Environmental Sciences, University of Tsukuba, 3058577
9 Ibaraki, Japan

10 2 Faculty of Agriculture, The University of Tokyo, 1138657 Tokyo, Japan

11 3 Graduate School of Agricultural and Life Sciences, The University of Tokyo,
12 1138657 Tokyo, Japan

13
14 *Corresponding Author, e-mail: hotta.norifumi.ge@u.tsukuba.ac.jp
15

16
17 **Abstract:** Debris flows include a great diversity of grain sizes resulting in inherent features
18 such as inverse grading, particle size segregation, and liquefaction of fine sediment. The
19 liquefaction of fine sediment affects the fluidity of debris flows, although the behavior and
20 influence of fine sediment in debris flows have not been examined sufficiently. This study used
21 flume tests to detect the effect of fine sediment on the fluidity of laboratory debris flows
22 consisting of particles with various diameters. From the experiments, the greatest sediment
23 concentration and flow depth were observed in the debris flows mixed with fine sediment
24 indicating increased flow resistance. The experimental friction coefficient was then compared
25 with the theoretical friction coefficient derived by substituting the experimental values into the
26 constitutive equations for debris flow. The theoretical friction coefficient was obtained from
27 two models with different fine-sediment treatments: assuming that all of the fine sediments
28 were solid particles or that the particles consisted of a fluid phase involving pore water
29 liquefaction. From the comparison of the friction coefficients, a fully liquefaction state was
30 detected for the fine particle mixture. When the mixing ratio and particle size of the fine
31 sediment were different, some other cases were considered to be in a partially liquefied
32 transition state. These results imply that the liquefaction of fine sediment in debris flows was
33 induced not only by the geometric conditions such as particle sizes, but also by the flow
34 conditions.
35

36 **Keywords:**

37 debris flow, fine sediment, friction coefficient, liquefaction, open channel, Reynolds stress
38

39 **Introduction**

40

41

42

43

44

45

46

47

48

49

50

The basic equations for debris flows have been derived from simple modeling of the laminar motion of sediment particles (Takahashi, 1977; Tsubaki *et al.*, 1982; Egashira *et al.*, 1997). These equations have been validated experimentally by comparing the theoretical and experimental velocity distributions (Takahashi, 1977; Egashira *et al.*, 1989; Itoh and Egashira, 1999) and the flow resistance (Arattano and Franzi, 2004; Hotta and Miyamoto, 2008). Debris flows have been classified into “boulder debris flows” or “stony debris flows”, and the interparticle stresses induced by particle-to-particle collisions and particle friction in the flow have been considered. In many cases, the particle size is assumed to be uniform and the mean diameter or d_{50} is used as a representative sediment particle size when applying these models to actual debris flows.

51

52

53

54

55

56

57

58

59

60

61

62

63

64

65

66

However, *in-situ* debris flows often include a great variety of grain sizes, including a relatively high portion of fine sediment. When debris flows contain a large amount of fine sediment, this sediment can affect the fluidity. Rickenmann (1991) and Takahashi and Kobayashi (1993) investigated the influence of fluid viscosity of clay suspensions on the fluidity of debris flows that consisted of clay and coarse particles, and found that the viscous coefficient of the pore fluid altered the total shear stress. In addition, Egashira *et al.* (1989, 1997) modeled a component of the shear stresses in the pore fluid of boulder debris flows as the Reynolds stress. Although sediment particles in the boulder debris flows, themselves, move laminar motion, the pore fluid should be turbulent because of the strong shear induced by the sediment particles. Hotta and Miyamoto (2008) pointed out that the friction coefficient in turbulent sediment flows was comparable with that of clear water; thus, the fine sediment contributes to the fluidity, even when the mass density of the interstitial fluid is increased without increasing the viscosity. Using the same concept, Nishiguchi *et al.* (2011) modeled debris flows with mixed grain sizes and large flow depths in which fine sediment was involved in the interstitial water; by doing so, they were better able to predict the run-out of large debris flows.

67

68

69

70

71

We conducted flume tests to detect the effect of fine sediment on the fluidity or the difference, due to different particle sizes of fine sediment in debris flows consisting of particles with mixed diameters. The experimental and theoretical flow resistances were then compared with those derived from experimental results to investigate the behavior of fine sediment.

72

1 Experiment

73

74

75

76

77

78

79

80

81

The variable slope channel of the Civil Engineering Research Laboratory (904-1 Tohigashi, Tsukuba, Ibaraki, Japan) was used for the experiments (Figure 1). The channel is 10 m long and 30 cm wide, with glazed sides. In these experiments, the width of the channel was reduced to 10 cm and the bottom of the lower stream of the channel (4.5 m) was raised as high as 10 cm. Sediment particles, 2.9 mm in diameter, were glued in the lower stream to provide bed roughness. An ultrasonic sensor (E4PA-LS50-M1, Omron, Kyoto, Japan) was installed 1 m above the lower end to measure the temporal change in the flow surface level at a sampling rate of 20 Hz.

82

83

The upper stream of the channel was filled with particles to a depth of about 10 cm. A steady flow of water was supplied from the upper end to generate a debris flow by eroding

84 sediment deposits in the upper section of the channel. The debris-flow sample was captured
 85 using a sampler at the downstream end, and the sampling time was recorded. The unit width
 86 flux Q and sediment flux concentration were obtained using the debris-flow sample. The
 87 debris-flow samples were obtained in the steady-state section, which could be verified by
 88 referring to the time series of the surface level data measured by an ultrasonic displacement
 89 sensor, as Hotta (2012) demonstrated using the same experimental setup. The average flow
 90 depth h was also obtained for the steady-state section, and the vertical (and cross-sectional)
 91 average flow velocity u_m was determined from the following relationship:

$$92 \quad Q = hu_m \quad (1)$$

93 Silica sands of five particle sizes were used in the experiments. Table 1 shows the
 94 particle sizes (mean diameter for 0.84–2.9 mm-sand and d_{50} for 0.11- and 0.23-mm sand) and
 95 the mixing ratio used in the experiments. The 0.84–2.9 mm sand was sieved to be as uniform
 96 as possible. The 2.9-mm sand was described as “large” particles. In addition to the two mixed
 97 diameters, tests were conducted using monogranular particles of the five sands. The mass
 98 density and interparticle friction angle of the sediment particles were 2.6 and 34°, respectively.
 99 The channel slope was set at 15°, and water was supplied from the upper end at about 3 Ls⁻¹.

100

101 **2 Analysis**

102 The friction coefficient f was used to compare the experimental results and the
 103 predicted values to examine the influence of fine sediment on fluidity. Here, experimental f
 104 was calculated using the following equation:

$$105 \quad f = \frac{2gh \sin \theta}{u_m^2} \quad (2)$$

106 where g is the acceleration due to gravity, h is the flow depth, θ is the channel slope, and u_m is
 107 the mean velocity.

108 The theoretical f for boulder debris flows over a rigid bed was obtained as follows.
 109 The energy dissipation (Φ) over a unit volume and time to achieve a steady debris flow is equal
 110 to the external energy supplied:

$$111 \quad \Phi = \rho_m gu \sin \theta \quad (3)$$

112 where ρ_m is the mass density of the debris flow and u is the velocity. Integrating Eq. (3) from
 113 the bed to the surface and substituting the result into Eq. (2) results in the following equations:

$$114 \quad \int_0^h \Phi dz = \int_0^h \rho_m gu \sin \theta dz = \rho_m gh u_m \sin \theta \quad (4)$$

$$115 \quad f = \frac{2gh \sin \theta}{u_m^2} = \frac{2}{\rho_m u_m^3} \int_0^h \Phi dz \quad (5)$$

116 Here, Φ can be rewritten as follows, based on the constitutive equations for debris flows
 117 proposed by Egashira *et al.* (1997):

$$118 \quad \Phi = K(c)d^2 \left(\frac{\partial u}{\partial z} \right)^3 \quad (6)$$

119 where d is the particle size, c is the volumetric sediment concentration, and $K(c)$ is an equation

120 expressed as a function of c . Refer to Hotta and Miyamoto (2008) for more detailed
121 information on $K(c)$.

122 To use the friction coefficient in our analysis, we postulated that the mixture of
123 sediment and water act as a single fluid, while sediment concentration in debris flow generally
124 differs according to the flow depth. In this study, a constant value was assumed for c , and the
125 velocity profile was assumed to be a typical velocity profile for boulder debris flows over a rigid
126 bed (Egashira *et al.*, 1989), which is also known as the velocity profile of a dilatant fluid
127 (Takahashi, 1977) and can be expressed as

$$128 \quad \frac{\partial u}{\partial z} = \frac{5u_m}{2h} \left(1 - \frac{z}{h}\right)^{1/2} \quad (7)$$

129 Then, f for debris flows can be obtained by substituting Eqs. (6) and (7) into Eq. (5) to obtain

$$130 \quad f = \frac{25}{2\rho_m} K(c) \left(\frac{h}{d}\right)^{-2} \quad (8)$$

131 Hotta and Miyamoto (2008) reported that the experimental and theoretical f corresponded
132 well for boulder debris flow in various flume tests, although the f value should be obtained for
133 steady-state, uniform sections of the debris flows.

134 In this study, two models were applied to calculate the theoretical friction coefficient
135 for the debris flows with sand of two mixed diameters, as shown in Figure 2. Model I assumed
136 that all of the fine (small) sediment acted as a solid phase; in this case, the sediment diameter
137 was calculated as a mean value using the large and small particle diameters. Conversely, Model
138 II assumed that all of the fine (small) sediment was involved in the interstitial water and acted
139 as a fluid phase. In Model II, the sediment diameter was set to that of the large particles (2.9
140 mm), the sediment concentration c was derived using only the large-sediment volume, and the
141 mass density of water ρ was calculated including the fine sediment. Note that a transition
142 between Models I and II is possible. In the transition state, fine sediment is partially involved
143 in the pore fluid showing the intermediate value of the friction coefficient between Models I
144 and II.

145

146 **3 Results and discussion**

147

148 **3.1 Experimental results**

149

150 Figure 3 shows the sediment concentrations in each experiment. The bars on the left
151 in all figures indicate the value for experiments carried out with uniform 2.9-mm particles. The
152 other three bars indicate the experiments carried out with mixing ratios of 1:4 and 1:1, and a
153 uniform particle experiment with small particles. The concentrations were divided into
154 concentrations of small and large particles, showing that the proportions were almost the same
155 as the initial mixing ratios. In the cases with 1.3- and 0.8-mm particles (Figure 3a, b), the total
156 sediment concentrations were almost the same as in the cases with uniform particle sizes.
157 However, the sediment concentration increased in the laboratory debris flows of mixed 0.2-
158 and 0.1-mm particles (Figure 3c, d). For a mixing ratio of 1:4, the concentration of large
159 (2.9-mm) particles was high enough to reach the concentration of debris flows with uniform
160 large (2.9-mm) particles.

161 Even when the fluxes of the laboratory debris flows were the same, the relationship
162 between flow depth and velocity varied with the flow conditions. Figure 4 shows the flow depth
163 for the experiments involving uniform particle sizes and mixed particles of two diameters. The
164 bars on the left show the flow depth for the experiment with uniform 2.9-mm particles. The
165 flow depth was greatest in the experiment with uniform 2.9-mm particles, as a consequence of
166 the greater flow resistance expressed in Eq. (8). Almost the same flow depth was observed in
167 the experiment with mixed 0.2- and 0.1-mm particles when the mixing ratio was 1:4.
168

169 **3.2 Comparison of the friction coefficients**

170

171 The modeled friction coefficients were compared with the experimental friction
172 coefficients, as shown in Figure 5. For the experiments with uniform particle sizes (Figure 5a),
173 both the experimental and theoretical friction coefficients were in good agreement for the
174 experiments with 2.9-mm particles. The theoretical friction coefficients were smaller for
175 smaller particles and were far from the experimental values for 0.23- and 0.11-mm particles. In
176 those experiments, the flow conditions were considered turbulent (Hotta and Miyamoto,
177 2008); however, the theoretical friction coefficient was derived from the constitutive equations
178 for boulder debris flows in which the flow is regarded as laminar, focusing on the sediment
179 particle motion.

180 In the experiments using mixed particle sizes, both Models I and II could not
181 sufficiently explain the experimental results. In Model I, the experimental and theoretical
182 friction coefficients were in good agreement for the 0.84-mm particles with a mixing ratio of
183 1:1 (Figure 5b) and for the 0.23-mm particles with a mixing ratio of 1:4 (Figure 5c). In Model II,
184 the experimental and theoretical friction coefficients were in good agreement for the 0.11-mm
185 particles with a mixing ratio of 1:1 (Figure 5d), and for the 0.11- and 0.23-mm particles with a
186 mixing ratio of 1:4 (Figure 5e). A comparison of the friction coefficients obtained from Models
187 I and II can be summarized as follows. The cases using the 0.84- and 1.3-mm particles alone or
188 the 0.23-mm particles with a mixing ratio of 1:4 were well described by Model I: small particles
189 were regarded as a solid phase. However, the friction coefficient of the 0.23-mm particles did
190 not differ significantly between Models I and II. Model II described well the case with the
191 0.11-mm particles with a mixing ratio of 1:4: the small particles acted as a fluid phase. The
192 cases with 0.11- and 0.23-mm particles with a mixing ratio of 1:1 showed intermediate values
193 or a better fit with Model II for the 0.11-mm particles. These cases suggest a transition from
194 Model I to II; i.e., fine sediment in the debris flows existed in both solid and fluid phases, and
195 there was a transition between the two phases depending on the flow conditions.

196 This idea was supported by the experimental results. As the sediment concentration
197 increased in cases with smaller particles (0.11 and 0.23 mm; Figure 3c, d), geometric
198 conditions such as the particle-diameter ratio allowed fine sediment to fill the pore spaces of
199 the coarse grains. When the mixing ratio was 1:4, the flow depth in cases with mixed particles
200 increased to approximate the flow depth in the experiment with uniform 2.9-mm particles
201 (Figure 4b). Assuming that different flow depths under the same conditions represent different
202 flow resistances, the friction coefficient is well described by Model II only when all of the fine
203 sediment is loaded in the interstitial space, such as with a mixing ratio of 1:4 (Figure 3c, d). In
204 this situation, internal stresses due to particle-to-particle collisions and friction in the debris
205 flow should mainly involve interactions among large particles. Such kinematic conditions can

206 probably allow us to regard the behavior of fine sediment in the interstitial space of large
207 particles as liquefaction.

208

209 **4 Conclusion**

210

211 This study conducted flume tests to detect the effect of fine sediment on the fluidity
212 of laboratory debris flows. The experiment used particles of two sizes: fine sediment consisting
213 of 0.11-, 0.23-, 0.84-, or 1.3-mm particles and coarse grains fixed at a size of 2.9 mm. From the
214 experiments, the greatest sediment concentration and flow depth were observed in the debris
215 flows with fine sediment containing 0.11- or 0.23-mm particles, indicating increased flow
216 resistance. The experimental and theoretical flow resistances were also derived from
217 experimental results to investigate the behavior of fine sediment. Comparing the friction
218 coefficients, complete liquefaction was observed in the experiment using 0.11-mm particles
219 with a mixing ratio of 1:4. The cases with 0.11-mm particles with a mixing ratio of 1:4, and both
220 0.11- and 0.23-mm particles with a mixing ratio of 1:1, were considered transition states. These
221 results infer that the liquefaction of fine sediment in debris flows was induced not only by the
222 geometric conditions, but also by the flow conditions such as internal stresses among sediment
223 particles. That is, it is possible that “fine sediment” and “coarse grains” in debris flows of
224 mixed particle sizes can be defined according to the kinematic conditions.

225

226 **Acknowledgments**

227

228 I sincerely thank Prof. Miyamoto (University of Tsukuba) for his comments on this
229 study. I also thank Mr. Sugiura and Mr. Hasegawa (Civil Engineering Research Laboratory,
230 Ibaraki, Japan) for their help with the experiments. This research was partially supported by
231 Grant-in-Aid for Scientific Research 22780140, 2010, from the Ministry of Education, Science,
232 Sports, and Culture, of Japan.

233

References

- Arattano M, Franzi L (2004) Analysis of different water-sediment flow processes in a mountain torrent. *Natural Hazard and Earth System Sciences* 4: 783-791.
- Egashira S, Ashida K, Yajima H, Takahama J (1989) Constitutive equations of debris flow. *Annals of the Disaster Prevention Research Institute, Kyoto University* 32 (B-2): 487-501. (in Japanese with English summary)
- Egashira S, Miyamoto K, Itoh T (1997) Constitutive equations of debris flow and their applicability. In: *Proceedings of the 1st International Conference on Debris-Flow Hazards Mitigation, San Francisco, California, US, 7–9 August 1997*. pp 340-349.
- Hotta N, Miyamoto K (2008) Phase classification of laboratory debris flows over a rigid bed based on the relative flow depth and friction coefficients. *International Journal of Erosion Control Engineering* 1 (2): 54-61.
- Hotta N (2012) Basal interstitial water pressure in laboratory debris flows over a rigid bed in an open channel. *Natural Hazards and Earth System Sciences* 12: 2499–2505.
- Itoh T, Egashira S (1999) Comparative study of constitutive equations for debris flows. *Journal of Hydroscience and Hydraulic Engineering* 17 (1): 59-71.
- Nishiguchi Y, Uchida T, Tamura K, Satofuka Y (2011) Prediction of run-out process for a debris flow triggered by a deep rapid landslide. In: *Debris-Flow Hazards Mitigation: Mechanics, Prediction and Assessment*, Genevois, R., Hamilton, D. L., Prestininzi, A. eds., Casa Editrice Universita La Sapienza, Roma. pp 477-485.
- Rickenmann D (1991) Hyperconcentrated flow and sediment transport at steep slopes. *Journal of Hydraulic Engineering* 117 (11): 1419-1439.
- Takahashi T (1977) A mechanism of occurrence of mud-debris flows and their characteristics in motion. *Annals of the Disaster Prevention Research Institute, Kyoto University* 20 (B-2): 405-435. (in Japanese with English summary)
- Takahashi T, Kobayashi K (1993) Mechanics of the viscous type debris flow. *Annals of the Disaster Prevention Research Institute, Kyoto University* 36 (B-2): 433-449. (in Japanese with English summary)
- Tsubaki T, Hashimoto H, Suetsugi T (1982) Grain stresses and flow properties of debris flows. In: *Proceedings of the Japan Society of Civil Engineers* 317: 79-91. (in Japanese)

Table 1 Particle sizes and mixing ratios used in the experiments. Large and small particles were mixed for experiments involving mixed diameters.

Small (mm)	Large (mm)	Mixing ratio
1.3		1:1
0.84	2.9	and
0.23		1:4
0.11		

Figure legends

Figure 1 Experimental setup.

Figure 2 Schematic diagrams of Models I and II. When the fine sediment is involved (liquefied) in the pore fluid, representative sediment particle size, sediment concentration, and density of the pore fluid change.

Figure 3 Sediment concentrations for the (a) 1.3-, (b) 0.84-, (c) 0.23-, and (d) 0.11-mm sediment particle experiments. Monogranular experiments and mixing ratios of 1:4 and 1:1 are shown in each column. The bars on the left in all figures indicate the sediment concentration for the uniform 2.9-mm particle experiments.

Figure 4 Flow depth for (a) uniform particle sizes and mixing ratios of (b) 1:4 and (c) 1:1. The bars to the left in (b) and (c) indicate the flow depth for the uniform 2.9-mm particle experiments as a reference.

Figure 5 Relationship between the experimental and theoretical friction coefficients for (a) uniform particle sizes (Model I), mixing ratios of (b) 1:1 and (c) 1:4 with Model I, and mixing ratios of (d) 1:1 and (e) 1:4 with Model II.

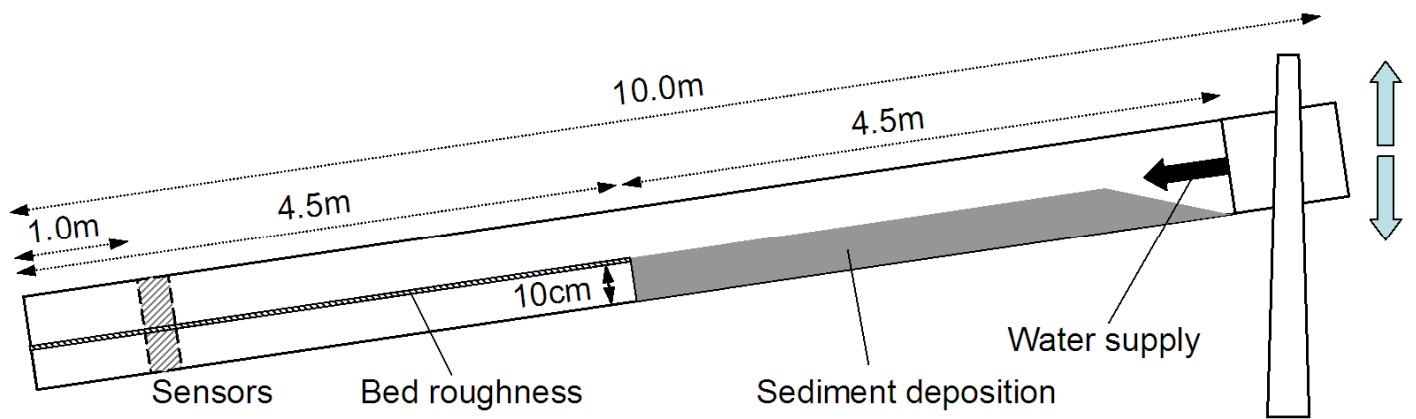


Figure 1 Experimental setup.

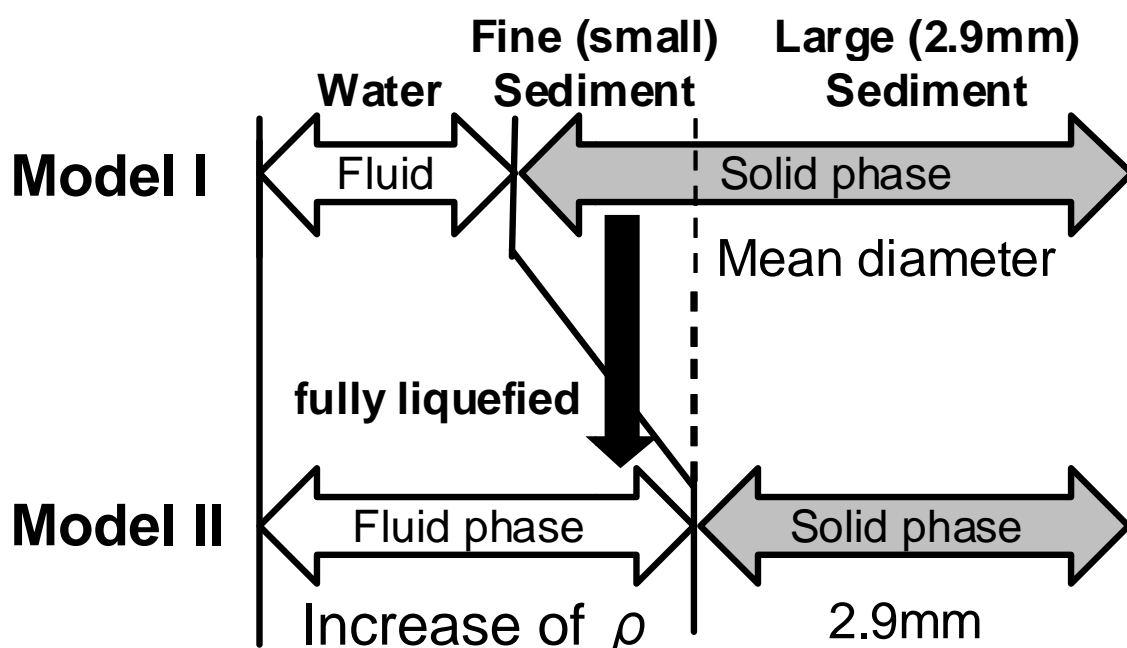


Figure 2 Schematic diagrams of Models I and II. When the fine sediment is involved (liquefied) in the pore fluid, representative sediment particle size, sediment concentration, and density of the pore fluid change.

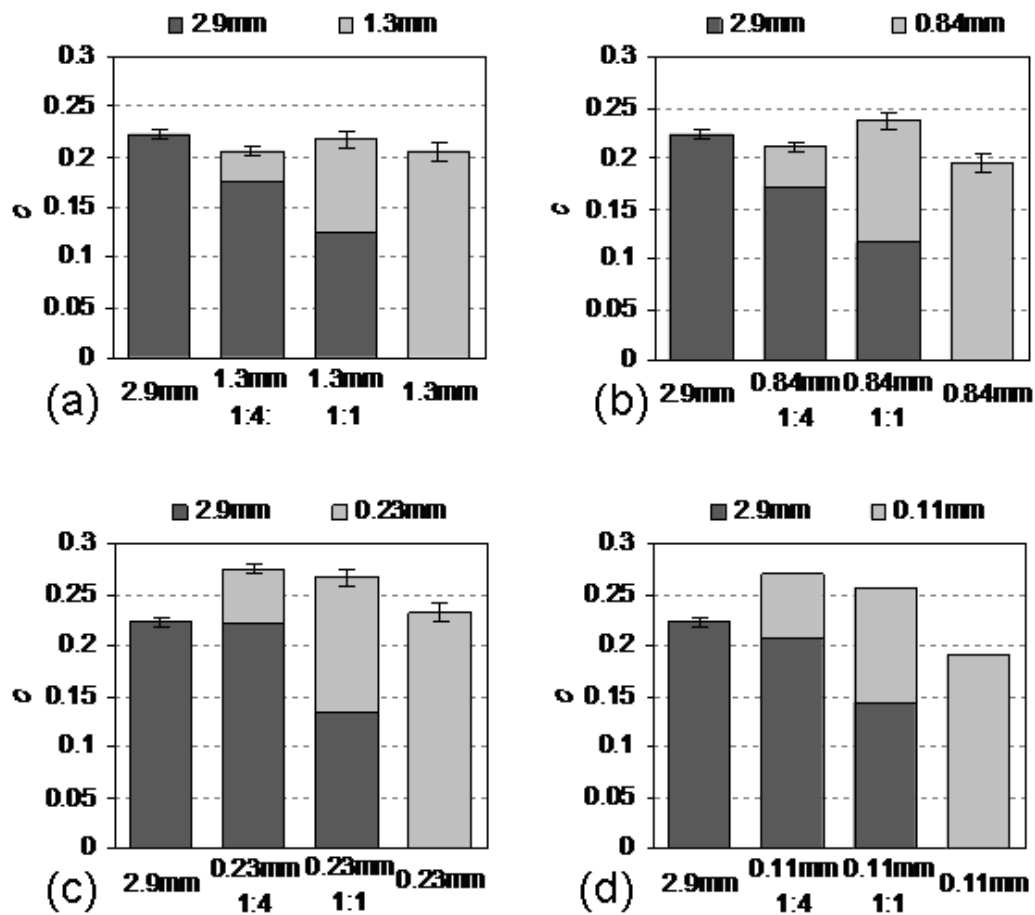


Figure 3 Sediment concentrations for the (a) 1.3-, (b) 0.84-, (c) 0.23-, and (d) 0.11-mm sediment particle experiments. Monogranular experiments and mixing ratios of 1:4 and 1:1 are shown in each column. The bars on the left in all figures indicate the sediment concentration for the uniform 2.9-mm particle experiments.

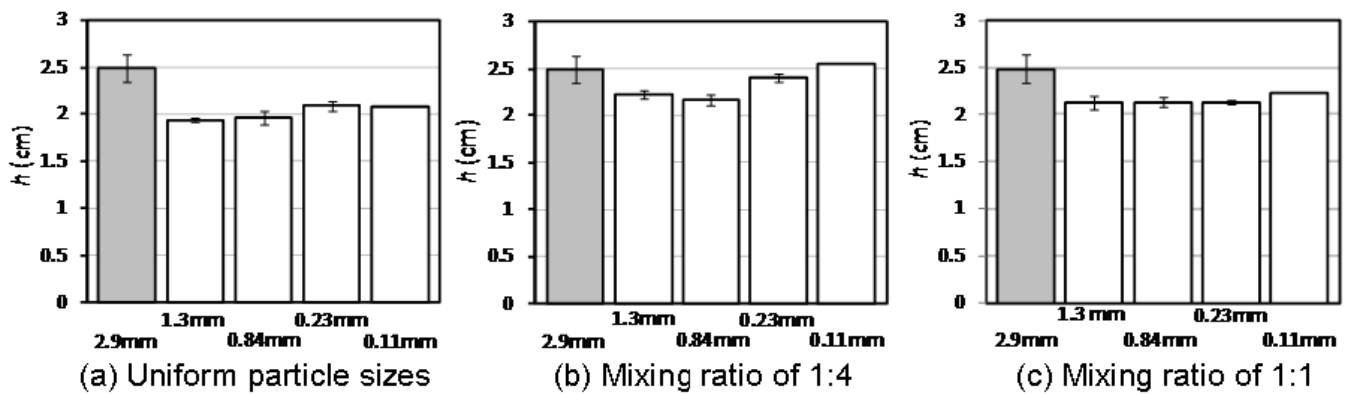


Figure 4 Flow depth for (a) uniform particle sizes and mixing ratios of (b) 1:4 and (c) 1:1. The bars to the left in (b) and (c) indicate the flow depth for the uniform 2.9-mm particle experiments as a reference.

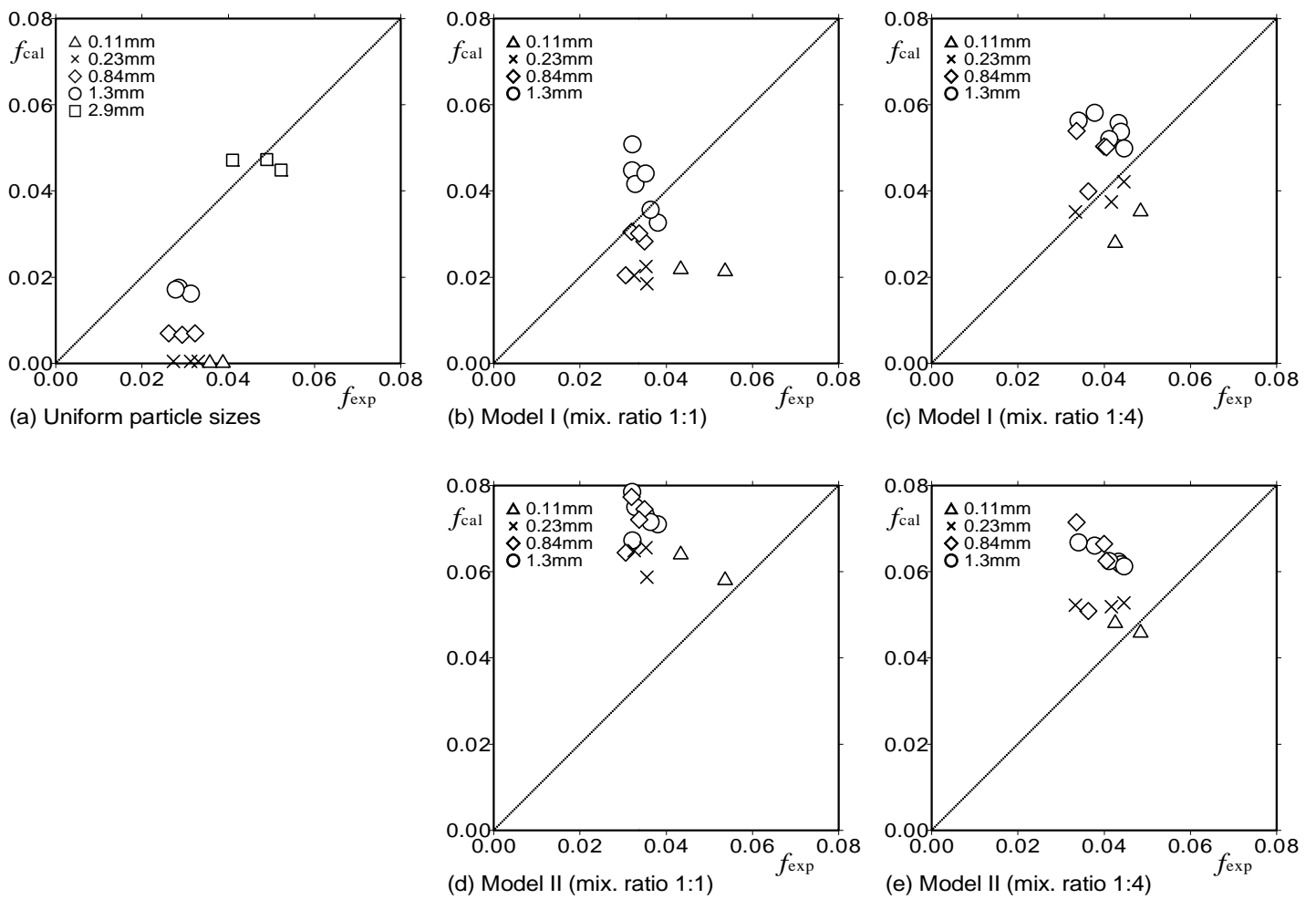


Figure 5 Relationship between the experimental and theoretical friction coefficients for (a) uniform particle sizes (Model I), mixing ratios of (b) 1:1 and (c) 1:4 with Model I, and mixing ratios of (d) 1:1 and (e) 1:4 with Model II.